

# Comparing the Topological and Electrical Structure of the North American Electric Power Infrastructure

Eduardo Cotilla-Sanchez\* and Paul D. Hines†

*School of Engineering, University of Vermont, Burlington, VT 05405, USA*

Clayton Barrows‡ and Seth Blumsack§

*John and Willie Leone Family Department of Energy and Mineral Engineering,  
The Pennsylvania State University, University Park, PA 16802*

## Abstract

The topological (graph) structure of complex networks often provides valuable information about the performance and vulnerability of the network. However, there are multiple ways to represent a given network as a graph. Electric power transmission and distribution networks have a topological structure that is straightforward to represent and analyze as a graph. However, simple graph models neglect the comprehensive connections between components that result from Ohm's and Kirchhoff's laws. This paper describes the structure of the three North American electric power interconnections, from the perspective of both topological and electrical connectivity. We compare the simple topology of these networks with that of random [1], preferential-attachment [2] and small-world [3] networks of equivalent sizes and find that power grids differ substantially from these abstract models in degree distribution, clustering, diameter and assortativity, and thus conclude that these topological forms may be misleading as models of power systems. To study the electrical connectivity of power systems, we propose a new method for representing electrical structure using electrical distances rather than geographic connections. Comparisons of these two representations of the North American power networks reveal notable differences between the electrical and topological structure of electric power networks.

---

\*Electronic address: eduardo.cotilla-sanchez@uvm.edu

†Electronic address: paul.hines@uvm.edu

‡Electronic address: cpb155@psu.edu

§Electronic address: sethb@psu.edu

## I. INTRODUCTION

Recent research in complex networks [4] has elucidated strong links between network structure and performance. Scale-free networks, which are characterized by strongly heterogeneous (power-law) node connectivity (degree), are uniquely robust to random failures but vulnerable to directed attacks [2, 5]. Graphs with exponential degree distributions, such as the random graph [1] and small-world networks [3] are more equally vulnerable to random failures and directed attacks. Scale-free networks also tend to lose synchronization when attacked at hub nodes [6], which is not the case for random graphs. And, for controllable networks, scale-free networks can be synchronized by controlling a small number of highly connected nodes [7], or even a single node [8]. On the other hand, ref. [9] shows that many classes of networks fail to synchronize, arguing that degree distribution alone is not sufficient to characterize the performance of a network. References [10, 11] describe how network structure influences consensus (a form of synchronization), and how different ways of representing a system a graph may affect the conclusions that one draws about performance. Others [12, 13] show that it is possible to maintain synchronization in evolving network topologies.

Given that network structure can dramatically influence performance, and given the size, complexity and importance of electric power systems, it is not surprising that power grids are the subject of substantial study from a complex networks perspective. The fact that data from many countries show a power-law in power system blackout sizes [14], leads naturally to the conjecture that this might result from complexity in network structure. Watts and Strogatz [3] measure characteristic path length and clustering in power grids, and find similarities to the small-world network model. A number of studies measure the degree distribution of various power grids with some reporting exponential [15, 16] and others reporting power-law/scale-free degree distributions [17, 18]. That studies of different power grids in different countries or regions yield different topological structures is not necessarily surprising. More surprising is that different analyses of identical grids (the transmission system in the Western U.S.) have yielded different structural results [16, 17]. This paper clarifies this uncertainty by showing that, at least for the IEEE 300 bus network and the US Eastern Interconnect, an exponential degree distribution is a better fit to the data than a power-law distribution. In addition to reporting an exponential degree distribution, ref. [16] also re-

ports a power-law in the topological betweenness of nodes in power grids, which is proposed as a potential explanation for the power-law blackout frequencies. Reference [19] compares the Western US power grid and the Nordic grid using the topological attack/failure model in [5], reports that the Nordic grid has a more heavy-tailed degree distribution structure than the Western grid, and provides some recommendations for increasing the robustness of power grids. Reference [20] studies the European power grid and finds a positive correlation between topological robustness measures and real non-topological reliability measures. Reference [21] uses results from a topological analysis to design a method for generating synthetic power grids.

While they provide some insight into network structure, these topological studies largely neglect Ohm’s and Kirchhoff’s laws, which govern flows in electric circuits. In some cases pure topological models can lead to provocative, yet erroneous, conclusions about network vulnerability [22]. To study electrical structure, refs. [23, 24] describe a measure of Electrical Centrality for power grids. Bompard et al. [25, 26] combine topological models with linearized power system models and propose new measures that can be useful in identifying critical components. Also using a power-flow model, ref. [27] identifies relationships between Wheatstone structures within power grids, reliability and efficiency.

### **A. Goals and outline of this paper**

This paper aims to fill a number of gaps in the existing research on the structure of electric power systems by identifying similarities and differences among the topological and electrical structure of power grids and synthetic networks. The data used for this study include several IEEE test cases, a 41,228 bus model of the US Eastern Interconnect (EI), a 11,432 bus model of the US Western Interconnect (WI), and a 4,513 bus model of the US Texas Interconnect (TI). These models are substantially more detailed, and accurate, than models that have been used in past structural studies of the North American power grid, including previous work by the authors [24].

Section II provides a topological analysis of the two networks, showing how power grids differ substantially from random [1], small world [3], and preferential attachment [2] graphs. Section III proposes a new method for studying power grids as complex networks, based primarily on electrical, rather than topological, structure. Section IV discusses some impli-

cations of these results for future studies of power grid performance.

## II. THE TOPOLOGICAL STRUCTURE OF POWER GRIDS

The existing literature shows some disagreement over the topological structure of power networks. Some report a power-law degree distribution [17, 18] whereas others argue that an exponential fit is superior [15, 16]. Several report that power grids have a small-world structure [3, 19, 28–30], from limited quantities of data. Some report that while the degree distribution is exponential (such as is the case with random graphs), power systems share properties with scale-free networks [16, 23, 31]. This section aims to clarify this and other uncertainties regarding the structure of power grids using a larger, more accurate model of the North American power grid than has been used in past studies. To determine the extent to which power networks are similar to or differ from common abstract network models, we compare the topology of the three US interconnections (West, East, and Texas) to similarly-sized small-world, scale-free and random graphs. This comparison builds on that in [21] by including a more comprehensive statistical description of not only power grids topology but also their counterpart canonical graphs and by utilizing a larger, more accurate representation of the North American power grid. Also, whereas ref. [21] focused on the generation of random test networks, our goal is to precisely describe the differences between topological and electrical structure.

To perform these comparisons, we represent each test network as an undirected, unweighted graph with  $n$  vertices/nodes and  $m$  links/edges. For the power grid models all buses, whether generator, load, or pass-through, are treated equally. In this representation, links can represent two or more parallel transformers or transmission lines, which means that  $m$  may be slightly smaller than the number of branches in the power system model. The set of all vertices and links in each graph,  $G$ , is  $\{N, M\}$ . The adjacency matrix for graph  $G_X$  is  $\mathbf{A}_X$ , with elements  $a_{ij}$ .

The following sub-sections describe the power grid data, the synthetic network models, and the metrics that are used for comparison purposes.

### A. Power grid data

The data used in this study include several standard test power systems (available from [32]), and a large model of the North American power grid composed by the US Eastern Interconnect (EI), US Western Interconnect (WI) and US Texas (ERCOT) Interconnect (TI). The Eastern Interconnect (EI) data come from a North American Electric Reliability Corporation (NERC) planning model for 2012. The Western and Texas data come from the FERC form 715 filings from 2005.[46]

The IEEE 300 bus test system has 411 branches, and average degree ( $\langle k \rangle = 2m/n$ ) of 2.73. Two of the branches are parallel links, so the graph size is:  $|G_{300}| = \{300, 409\}$ . After removing isolate buses and parallel branches from the EI data we obtain a graph ( $G_{EI}$ ) with 41,228 vertices, 52,075 links and an average degree  $\langle k \rangle = 2.53$ . After applying the same process to  $G_{WI}$  we obtain a graph with 11,432 vertices, 13,734 links and an average degree  $\langle k \rangle = 2.40$ . For the Texas Interconnection  $|G_{TI}| = \{4513, 5532\}$  and  $\langle k \rangle = 2.45$ .

### B. Synthetic networks

In order to compare power grids to common graph structures, we synthesized similarly sized graphs using the small-world [3], preferential attachment (scale-free) [2], and random [1] graph models, each of which is described below.

The early work on small-world networks [3] argues that power networks have the properties of a small-world system. Others also report this to be true [19, 28–30]. To test whether this is indeed the case we generate a regular lattice with  $n$  nodes and approximately  $m$  links. Nodes and links are initially laid out to form a ring lattice, by forming links to neighboring nodes, such that each node  $a$  is connected  $a \leftrightarrow a - 1$  ( $\forall a > 1$ ). A second link is then created from node  $a$  to node  $a - 2$  (for  $a > 2$ ) with probability  $\text{Pr}(a \leftrightarrow a - 2) = m/n - 1$ , giving approximately  $m$  links in total. After generating the regular lattice in this manner, random re-wiring proceeds for each node with probability  $p$  as in [3]. We adjust  $p$  to obtain a network with the same diameter as the corresponding power grid.

Similarly, several [17, 18] argue that power grids have a scale-free structure, as evidenced by a power-law in the degree distribution. As with the small-world network we synthesize scale-free networks to match the size of each power network. To create a preferential

attachment/scale-free (PA) graph with roughly  $n$  nodes and  $m$  links we modify the algorithm described in [2] to allow for a fractional average degree  $\langle k \rangle$ . For each new node  $a$  we initially add one link between  $a$  and an existing node  $b$  using the standard roulette wheel method. Specifically, node  $b$  is selected randomly from the probability distribution  $\Pr(a \leftrightarrow b) = k_b / \sum_{c=1}^n k_c$ , where  $k_c$  is the degree at node  $c$ . After adding this initial link a second is added with probability  $m/n - 1$ . Thus the addition of each new node results in an average of  $1 + (m/n - 1) = m/n$  new links, producing a preferential attachment graph with  $n$  nodes and roughly  $m$  links.

Finally, we synthesize random graphs by randomly linking node pairs until there are exactly  $m$  links in the system.

### C. Measures of graph structure

If one of the above abstract models is a good model for power networks, then statistical measures for the synthetic graphs should be similar to those that come from the power networks. There are many useful statistical measures for graphs. Among the most useful are degree distribution [2], characteristic path length [3], graph diameter [33], clustering coefficient [3] and degree assortativity [2]. These measures provide a useful set of statistics for comparing power grids with other graph structures.

The probability mass function (pmf) for node connectivity, or degree distribution, describes the diversity of connectivity in a graph. While random graphs have an exponential (single scale) degree distribution, many real networks have a power-law degree distribution. These scale-free networks tend to have highly connected hubs, which can make the network vulnerable to directed attack [5]. The degree of node  $i$  in a graph with adjacency matrix  $A$  is:

$$k_i = \sum_{j=1}^n a_{ij} \quad (1)$$

and the degree distribution is  $\Pr(k = x) = n_k/n$ , where  $n_k$  is the number of nodes with degree  $k$ . The complementary cumulative distribution function (ccdf) of degree in a scale-free network will follow a power-law function:

$$\Pr(k \geq x) = \left( \frac{x}{x_{\min}} \right)^{-\alpha+1} \quad (2)$$

where  $x_{\min}$  is a minimum value for the power-law tail of the degree distribution. If the degree distribution is exponential, a minimum value Weibull distribution provides a better fit to the data:

$$\Pr(k \geq x) = e^{-\left(\frac{x-x_{\min}}{\lambda}\right)^\beta}. \quad (3)$$

While the size of a network can be measured by the number of nodes,  $n$  does not give much information about distances within the network, which are often an indicator of network performance. Two measures of network distance are commonly employed: diameter ( $d_{\max}$ ) and characteristic path length ( $L$ ). If  $\mathbf{D}$  is a distance matrix, in which the off-diagonal elements  $d_{ij}$  give the minimum number of links that one would need to traverse to get from node  $i$  to node  $j$ , then the diameter of the network is:

$$d_{\max} = \max_{ij} d_{ij}. \quad (4)$$

The characteristic path length ( $L$ ) is the average of all  $d_{ij}$ :

$$L = \frac{1}{n(n-1)} \sum_{\substack{\forall i,j \\ i \neq j}} d_{ij} \quad (5)$$

The manner in which a type of network increases in diameter ( $L$  or  $d_{\max}$ ) is a useful indicator of structure. In small-world networks and random graphs,  $L$  increases roughly with  $\ln n$  [3], which gives these networks their characteristically small distances between vertices. In a circular lattice  $L$  increases linearly with  $n$ , and in a regular 2-dimensional grid  $L$  will increase with  $\sqrt{n}$ . Small-world networks differ from random graphs in that nodes in small-world graphs are highly clustered, as they are in regular lattice or grid structures [3]. Therefore if power networks were small-world in structure, we would expect to see high clustering and small distances. Section II D describes an asymptotic analysis of  $L$  for several power grids, which indicates that power grids fall somewhere between small-world and regular network structures. In this paper clustering is measured with the clustering coefficient described in [3]:

$$C = \frac{1}{n} \sum_{i=1}^n c_i \quad (6)$$

where the clustering of node  $i$  ( $c_i$ ) is

$$c_i = \frac{e_i}{(k_i(k_i - 1))/2} \quad (7)$$

and  $e_i$  is the number of links within the cluster of nodes including node  $i$  and its immediate neighbors  $N_i$ :

$$e_i = \sum_{\forall j,k \in \{N_i \cup i\}} a_{jk}/2 \quad (8)$$

Finally we compare the degree assortativity in the test networks. Degree assortativity ( $r$ ) in a network is defined in [34] as the extent to which nodes connect to nodes with similar degree. Formally, assortativity is the correlation in degree for the nodes on opposite ends of each link [35]:

$$r = \frac{m^{-1} \sum_{i=1}^m j_i k_i - [m^{-1} \sum_{i=1}^m \frac{1}{2}(j_i + k_i)]^2}{m^{-1} \sum_{i=1}^m \frac{1}{2}(j_i^2 + k_i^2) - [m^{-1} \sum_{i=1}^m \frac{1}{2}(j_i + k_i)]^2} \quad (9)$$

where  $m$  is the number of links in the network and  $j_i/k_i$  are the degrees of the endpoints of link  $i$ .

#### D. Topological results

Our analysis of the IEEE 300 bus and the North American power grid models clearly indicates that power networks are neither small world, nor scale-free in structure. Two hypothesis tests regarding degree distribution provide evidence for this conclusion. Hypothesis 1 is that the power networks have the same degree distribution as the same-sized synthetic network ( $\Pr(k) \sim \Pr(k : \text{EI})$ ). Hypothesis 2 is that various networks have a power-law degree distribution ( $\Pr(k) \sim k^{-\alpha}$ ). We use a Kolmogorov-Smirnov t-test to evaluate each hypothesis. For hypothesis 2, we determine the power-law distribution fit parameters ( $\alpha$  and  $x_{\max}$ ) using the method described in [36]. Table I shows results from these tests, as well as other measures of network structure.

Tests of hypothesis 1 indicate that the degree distributions of the power networks do not match those of the synthetic networks in all but one case: the IEEE 300 network compared to a random graph. In Fig. 1, which shows the degree distributions for the large graphs, it is clear that high-degree nodes are more frequent than would be found in random graphs or small-world networks, but far less frequent than would be found in a similarly sized scale-free network. Hypothesis 1 can be rejected with high confidence.

The tests of hypothesis 2 show, with high confidence, that none of the North American power network degree distributions follow a power-law ( $P < 0.001$ ). The power-law



Table I: Comparison between power grid models and synthetic networks

| Network             | Power network |          |          |         | Random        |          |          |          | Small world |          |          |          | Preferential attachment |               |               |               |
|---------------------|---------------|----------|----------|---------|---------------|----------|----------|----------|-------------|----------|----------|----------|-------------------------|---------------|---------------|---------------|
|                     | IEEE          | EI       | WI       | TI      |               |          |          |          | $p =$       | $p =$    | $p =$    | $p =$    |                         |               |               |               |
|                     | 300           |          |          |         |               |          |          |          | 0.08        | 0.0882   | 0.18     | 0.22     |                         |               |               |               |
| Nodes               | 300           | 41228    | 11432    | 4513    | 300           | 41228    | 11432    | 4513     | 300         | 41228    | 11432    | 4513     | 300                     | 41228         | 11432         | 4513          |
| Links               | 409           | 52075    | 13734    | 5532    | 409           | 52075    | 13734    | 5532     | 402         | 52209    | 13737    | 5527     | 409                     | 52032         | 13719         | 5521          |
| $\langle k \rangle$ | 2.73          | 2.53     | 2.40     | 2.45    | 2.73          | 2.53     | 2.40     | 2.45     | 2.68        | 2.52     | 2.40     | 2.45     | 2.73                    | 2.52          | 2.40          | 2.45          |
| $\max(k)$           | 11            | 29       | 22       | 18      | 7             | 12       | 11       | 11       | 6           | 6        | 6        | 6        | 32                      | 419           | 185           | 125           |
| $C$                 | 0.11          | 0.068    | 0.073    | 0.031   | 0.008         | 0.00008  | 0.00015  | 0.0001   | 0.26        | 0.26     | 0.16     | 0.15     | 0.008                   | 0.00054       | 0.002         | 0.004         |
| $L$                 | 9.9           | 31.9     | 26.1     | 14.9    | 5.7           | 11.2     | 10.3     | 9.02     | 9.6         | 34.2     | 22.9     | 16.9     | 4.4                     | 7.1           | 6.8           | 6.1           |
| $d_{\max}$          | 24            | 94       | 61       | 37      | 12            | 27       | 24       | 20       | 24          | 101      | 59       | 41       | 9                       | 17            | 17            | 15            |
| $r$                 | -0.22         | -0.10    | -0.08    | -0.09   | 0.044         | 0.004    | -0.01    | -0.03    | 0.034       | 0.12     | 0.052    | 0.03     | -0.19                   | -0.03         | -0.05         | -0.09         |
| Hyp. 1              | -             | -        | -        | -       | not<br>reject | reject** | reject** | reject** | reject**    | reject** | reject** | reject** | reject**                | reject**      | reject**      | reject**      |
| Hyp. 2              | mar-<br>ginal | reject** | reject** | reject* | reject*       | reject** | reject** | reject** | reject**    | reject*  | reject** | reject** | not<br>reject           | not<br>reject | not<br>reject | not<br>reject |
| est. of $\alpha$    | 3.5           | 3.35     | 3.33     | 3.44    | 3.5           | 3.5      | 3.5      | 3.5      | 3.5         | 3.29     | 3.42     | 3.25     | 2.49                    | 2.8           | 2.92          | 2.55          |

\* Significant at the 0.01 confidence level.

\*\* Significant at the 0.001 confidence level.

exponents found ( $\alpha = 3.33$  to  $\alpha = 3.5$ ) are steeper than what would generally be considered notable power-law distributions [36]. As expected the scale-free network fits well with a power-law degree distribution. These results lead us to conclude, with confidence, that power networks are not scale-free in topological structure.

The conjecture that power networks are small-world in structure requires some additional analysis. While the clustering coefficients of the power grids are less than those of the small-world graphs,  $C$  is an order of magnitude higher in power grids than in random networks (table I). To test whether the small-world model is a good model for power grids, we introduce a third hypothesis. Hypothesis 3 is that the characteristic path lengths of power grids increase with an upper bound of  $L \leq \ln n$ , which is argued in [3] and [4] to be the limit for distances in small-world networks. Figure 2 compares the characteristic path

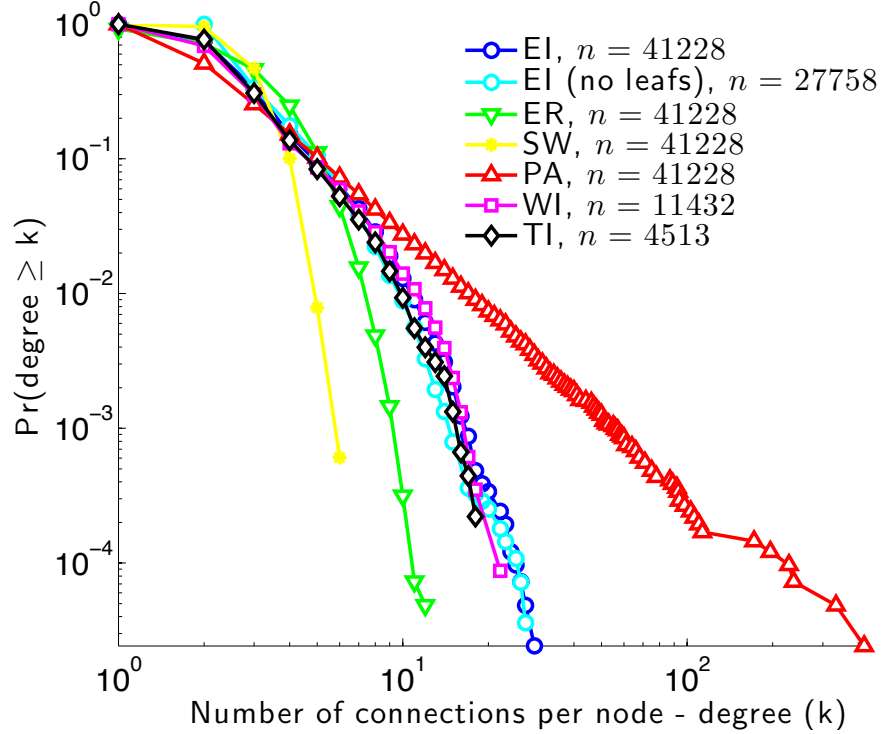


Figure 1: Cumulative degree distributions of the Eastern (EI), Western (WI) and Texas (TI) interconnections, along with degree distributions for synthetic networks sized to match EI:  $|G_{EI}| = \{41228, 52075\}$ . Power networks have a heavy-tailed, but not power-law (scale-free) degree distribution.

lengths of several power networks with predicted values for  $L$  from the small-world, scale-free, and random graph models. Path lengths in large power grids increase substantially faster than  $\ln n$ , which means that power grids fall somewhere between a regular grid, in which path lengths scale linearly with  $n$  or  $\sqrt{n}$ , and a small-world network. Because  $L > \ln n$  for all of the power networks of substantial size ( $n > 30$ ) hypothesis 3 can be safely rejected. Therefore, methods that are based on the assumption that power grids belong to the small-world family of networks (e.g., [30]) may be misleading.

A number of other results in table I and Fig. 1 are notable. The small world networks had much higher clustering than the power networks, largely because the re-wiring probabilities ( $p$ ) were chosen to keep distances similar to those found in the power networks, and were thus very small. That the power networks had a fairly high degree of clustering may be the result of geographic constraints that make very long-distance connections impractical in most cases. Also we find that power networks have a small, negative degree assortativity.

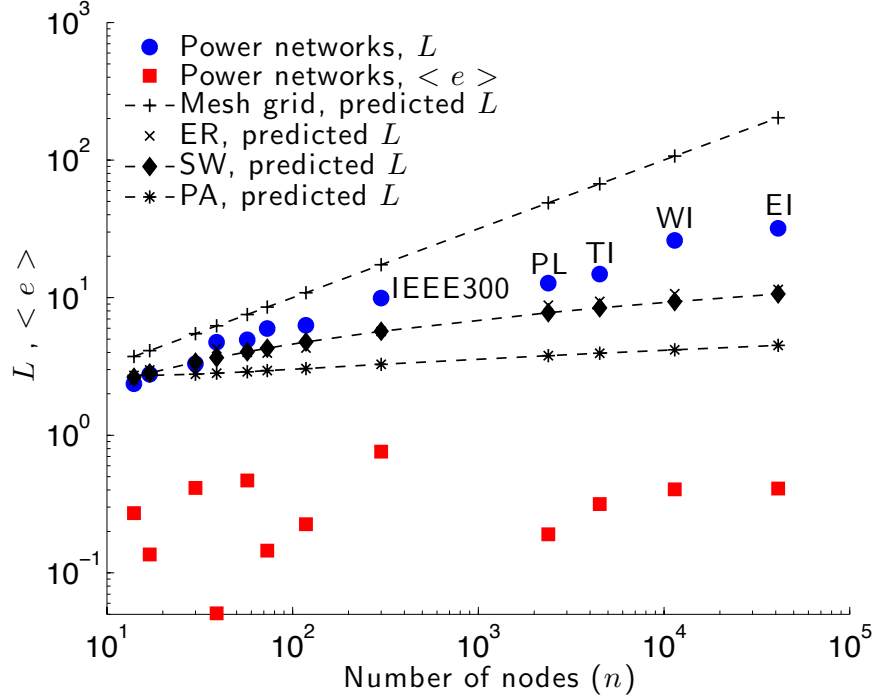


Figure 2: Characteristic path length ( $L$ ) and average electrical distance ( $\langle e \rangle$ ) of the power networks as a function of graph size,  $n$ .  $L$  increases faster than  $\ln n$  in the power networks, which indicates that the small-world model does not fit particularly well. PL is the test system “case2383wp” from [37]. The smaller networks are standard IEEE test cases, also available from [37].

In contrast, the small-world model shows a positive degree correlation, and, as expected, the preferential-attachment and random graph models show nearly zero assortativity. The negative assortativity in the power networks was found to result from substation buses with a large number of radial connections (typically distribution feeders). If the degree-1 “leaf nodes” are recursively removed the assortativity becomes very nearly zero. Upon recalculating the assortativity of EI, WI and TI after removing the leaf nodes, we find the following changes in assortativity: EI, from  $r = -0.10$  to  $-0.02$ ; WI, from  $r = -0.08$  to  $-0.01$ ; and TI, from  $r = -0.09$  to  $-0.02$ .

### III. THE ELECTRICAL STRUCTURE OF POWER GRIDS

While a thorough understanding of topological structure can be useful for some problems, such as producing synthetic power grids [21], data about topological structure are not sufficient to describe the performance of power networks [22]. The structure of a power grid

depends not only on its topology, but also on the relationships that results from the physical properties that govern flow. To understand the electrical structure of a given power grid we need a measure of electrical connectedness, or conversely distance. Electrical distance has been used in a number of power systems problems [38–41], although it has not been used to compare the electrical and topological properties of power networks.

To qualify as a distance metric, a metric space  $d(x, y)$  must map pairs of elements in a set in a way that describes the dissimilarity among any element  $(x, y, z)$ , and must have the properties of non-negativity ( $d(x, y) \geq 0$ ), symmetry ( $d(x, y) = d(y, x)$ ), identity ( $d(x, y) = 0 \Leftrightarrow x = y$ ) and the triangle inequality ( $d(x, z) \leq d(x, y) + d(y, z)$ ) [42]. Reference [38] showed that the logarithmic voltage magnitude sensitivity in a power grid can qualify as a distance metric, under some conditions. In this paper we use a distance metric based on the relationship between electric power transactions that occur in a power grid and the voltage phase-angle differences between points in the grid, which is a common measure of stress in power systems [43]. To do so we start with a network of resistors with current injections at each node which can be described by a conductance matrix  $\mathbf{G}$ , such that the current injection at node  $a$  is:

$$I_a = \sum_{b=1}^n g_{ab} V_b \quad (10)$$

When there are no connections to ground in the circuit,  $\mathbf{G}$  has rank  $n - 1$ , unless a voltage reference is specified. To get around the singularity of  $\mathbf{G}$ , we let node  $r$  be a voltage reference node, with  $V_r \triangleq 0$ . The sub-matrix of  $\mathbf{G}$  associated with the non-reference nodes ( $\bar{r}$ ) is full-rank, therefore we can compute a sub-matrix  $\mathbf{G}_{\bar{r}\bar{r}}^{-1}$ , such that:

$$\mathbf{V}_{\bar{r}} = \mathbf{G}_{\bar{r}\bar{r}}^{-1} \mathbf{I}_{\bar{r}}. \quad (11)$$

If the diagonal element of  $\mathbf{G}_{\bar{r}\bar{r}}^{-1}$  associated with node  $a$  is  $g_{a,a}^{-1}$ ,  $g_{a,a}^{-1}$  indicates the change in voltage between nodes  $a$  and  $r$  as a result of a current injection at node  $a$ , which must be withdrawn from node  $r$ . Thus the electrical distance between  $a$  and  $r$  is  $g_{a,a}^{-1}, \forall a$ . To measure the distance between nodes  $a$  and  $b$ , where  $a \neq b \neq r$ , one can evaluate:

$$e(a, b) = g_{a,a}^{-1} + g_{b,b}^{-1} - g_{a,b}^{-1} - g_{b,a}^{-1}, \quad (12)$$

which gives the voltage difference between  $a$  and  $b$  after injecting 1 A at  $a$  and withdrawing 1 A from  $b$ . In matrix form, where  $\gamma \triangleq \text{diag}(\mathbf{G}_{\bar{r}\bar{r}}^{-1})$ , the calculation proceeds efficiently as

follows:

$$\mathbf{E}_{\bar{r}\bar{r}} = \mathbf{1}\gamma^T + \gamma\mathbf{1}^T - \mathbf{G}_{\bar{r}\bar{r}}^{-1} - [\mathbf{G}_{\bar{r}\bar{r}}^{-1}]^T \quad (13)$$

$$\mathbf{E}_{r,\bar{r}} = \gamma^T \quad (14)$$

$$\mathbf{E}_{\bar{r},r} = \gamma \quad (15)$$

where  $\mathbf{E}_{\bar{r},r}$  refers to vector of non-reference elements in the reference column of the distance matrix. When  $\mathbf{G}$  is a real-valued conductance matrix, this distance is known as a “Resistance Distance” and is proven to have the properties of a metric space in [44]. In ac circuits, voltages and currents are represented with phasor quantities, therefore this definition of distance needs some modification. To produce a real-valued distance metric for a power system we replace the conductance matrix  $\mathbf{G}$  with the quadrant of the power flow Jacobian that represents the sensitivity of average power injections,  $P$ , to changes in nodal phase angles,  $\theta$ :

$$\Delta\mathbf{P} = \left[ \frac{\partial P}{\partial \theta} \right] \Delta\theta.$$

Applying (12) with  $\mathbf{G} = [\partial P / \partial \theta]$  results in a distance matrix ( $\mathbf{E}$ ) that measures the incremental change in phase angle difference between nodes  $a$  and  $b$  ( $\theta_a - \theta_b$ ) given an incremental average power transaction between nodes  $a$  and  $b$ . As in [38], we empirically find that  $\mathbf{E}$ , thus defined, satisfies the properties of a distance matrix so long as all series branch reactances are non-negative, which would be the case with transmission lines with large series capacitors (see appendix).

Using this metric we can define a measure that is roughly analogous to node degree, but for a fully connected network with continuous weights for each node pair. To do so we measure the average distance from each node  $a$  to other nodes in the system:

$$\langle e_a \rangle = \sum_{b=1}^n \frac{e_{ab}}{n-1} \quad (16)$$

and invert it to obtain a measure of electrical centrality (modified from [23]):

$$c_a = \frac{1}{\langle e_a \rangle}. \quad (17)$$

The lower panel of Fig. 3 illustrates the electrical centrality of buses in the IEEE 300 bus system, which shows a group of nodes with very high electrical connectivity, and the majority of nodes showing minimal centrality.

Electrical distances are notably different than topological distances. Figure 5 shows that there is only a very weak correlation between electrical and topological distances ( $\rho = 0.24$  for  $\langle e_a \rangle$  and  $\langle d_a \rangle$ ). Many node pairs that are close topologically are distant in terms of electrical distance. It is notable that the correlation is stronger at the higher (500kV and 765kV) voltage levels where there is less diversity in branch impedances. Figure 4 compares the distribution of electrical and topological distances obtained from the EI, WI and TI models. Furthermore, the topological distance distributions (**D**) have exponential tails, whereas the electrical distance distributions (**E**) have power-law tails.

The electrical distance matrix can be used to produce a graph representation of the electrical structure of a power network. To do so, we keep the original  $n$  nodes, but replace the  $m$  links with the  $m$  smallest entries in the upper (or lower since **E** is symmetric) triangle of **E**. Thus we create a graph of size  $\{n, m\}$  with links representing strong electrical connections rather than direct physical connections. The adjacency matrix of this new graph (**R**) is defined as follows:

$$\mathbf{R} : \begin{cases} r_{ab} = 1 & \forall e_{ab} < t \\ r_{ab} = 0 & \forall e_{ab} \geq t \end{cases}$$

where  $t$  is a threshold adjusted to produce exactly  $m$  links in the network. Figure 3 shows the electrical structure (**R**) for the IEEE 300 bus test case. Comparison of the topology (**A** in Fig. 3) to the electrical structure (**R** in Fig. 3) shows a stark contrast between the electrical and topological structure of the test system. A similar structural difference is found by comparing the topology and electrical structure of North American systems. Table II summarizes the calculated metrics for the Eastern Interconnection **R** matrix. Electrically speaking, a few nodes have a very high connectivity, whereas the vast majority of vertices in **R** have no connections, which is to say that power systems are electrically similar to the scale-free network model. The clustering coefficient of **R** is also high relative to the value obtained from the equivalent topological network. Both path lengths ( $L$ ) and diameter ( $d_{\max}$ ) are smaller in the electrical graph, indicating strong electrical connectedness within the core. The WI and TI electrical networks are highly disassortative ( $r < 0$ ), whereas the EI system is electrically assortative ( $r = 0.33$ ).

Table II: Topologically equivalent metrics for the reduced electrical distance matrices ( $\mathbf{R}$ ).\*

| Network             | EI ( $\mathbf{R}$ ) | EI ( $\mathbf{A}$ ) | WI ( $\mathbf{R}$ ) | WI ( $\mathbf{A}$ ) | TI ( $\mathbf{R}$ ) | TI ( $\mathbf{A}$ ) |
|---------------------|---------------------|---------------------|---------------------|---------------------|---------------------|---------------------|
| Nodes**             | 41228 (56)          | 41228               | 11432 (8017)        | 11432               | 4513 (2769)         | 4513                |
| Links               | 52075               | 52075               | 13734               | 13734               | 5532                | 5532                |
| $\langle k \rangle$ | 2.53                | 2.53                | 2.40                | 2.40                | 2.45                | 2.45                |
| $\max(k)$           | 41171               | 29                  | 3413                | 22                  | 762                 | 18                  |
| $C$                 | 0.9996              | 0.068               | 0.9982              | 0.073               | 0.49                | 0.031               |
| $L$                 | 1.999               | 31.9                | 1.998               | 26.1                | 2.79                | 14.9                |
| $d_{\max}$          | 2                   | 94                  | 3                   | 61                  | 13                  | 37                  |
| $r$                 | 0.33                | -0.10               | -0.96               | -0.08               | -0.29               | -0.09               |

\* Metrics are calculated for the giant component.

\*\* Numbers in parenthesis account for isolated nodes.

### A. Electrical distance to load

The distance metric described by (11)-(13) gives sensitivities between arbitrary node pairs in a power network. We can refine this metric to focus on electrical distances from an arbitrary node to load nodes. This "electrical distance to load" measure describes the sensitivity of consumption nodes to perturbations at other locations in the network. In this section we determine the electrical distance to load of approximately 5600 buses within the US mid-Atlantic (PJM) portion of the EI model. From the electrical distance matrix,  $\mathbf{E}$ , we plot (Fig. 6) the amount of the total system load that is reachable at various electrical distances. Comparing this to a similar graph for topological distances illustrates the difference between the two. Topologically there are a few nodes that are within 1 link ( $d_{ab} \leq 1$ , or 5.3% of the topological diameter,  $d_{\max}$ ) of about 2 GW of load, which is 1% of the total system load of 146.8 GW (lower panel of Fig. 6). Electrically, there are a few nodes that are within  $e_{ab} \leq 0.011$  (0.5% of the electrical diameter,  $e_{\max}$ ) of 40 GW (27%) of load. This indicates that a small number of nodes have a very high electrical influence on the system as a whole. Typically, these are high voltage buses (500kV and larger) that show very high electrical centrality.

## IV. CONCLUSIONS

Power grids have been an appealing topic for network analysis in recent years, but the existing body of literature has produced some mixed results, particularly related to measuring the structure of power networks and connections between structure and performance. We have assessed the topological structure of the North American electric power network, and have compared it with a structural analysis based on a measure of “electrical distance,” which measures network sensitivities. Electrical distance is more closely related to the physical laws governing behavior in electrical networks than topological distance or connectivity. In the appendix we show the conditions under which the proposed distance measure qualifies as a formal distance metric. Simpler impedance-based measures of electrical distance used elsewhere in the literature do not always meet the criteria for a proper distance metric.

Our analysis of the topological structure of the Eastern, Western and Texas Interconnects clearly suggests an exponential degree distribution rather than a power-law. We thus reject the conjecture that the observed power-law distribution in blackout sizes arises due to a power-law in the grid topology. Further, we observe significant differences between power-grid topologies and the topology of synthetic small-world networks. Distances between nodes increase much faster than the log of network size, and clustering is not as high as is found in true small-world networks. On a topological basis, we thus conclude that power grids are neither scale-free nor small-world in topological structure.

When we measure network structure based on electrical distance, however, we find a power-law distribution in electrical distances for all three Interconnects in the North American power network. The correlation between electrical and topological distance is weak, though it increases for higher-voltage lines. When we look at the electrical distances to load in the system, we find that a small number of nodes are tightly electrically connected to large percentages of load in the system, despite being relatively distant topologically. Since our electrical distance measure captures network sensitivities rather than physical connectivity, the observed heterogeneous structure suggests that perturbations (such as those caused by a volitional attack or changes in generator pricing) may have non-local effects more often than would be expected from the grid’s topological structure. Our work suggests that future endeavors to relate structure and performance in electrical networks should focus on characterizing network sensitivities rather than focusing on topological connectivity.



## Appendix. Conditions under which electrical distance qualifies as a formal distance measure

Equations (12)-(13) describe our measure of electrical distance  $e(a, b)$ , given a sensitivity matrix  $\mathbf{G}$ . Here we discuss the conditions under which  $e(a, b)$  qualifies as a proper distance metric in some metric space. Following [42, 44], a distance metric  $e(\cdot)$  on an arbitrary metric space satisfies the following properties, for all  $a, b, c$ :

- Symmetry:  $e(a, b) = e(b, a)$
- Identity:  $e(a, b) = 0 \iff a = b$
- Non-Negativity:  $e(a, b) \geq 0$
- Triangle Inequality:  $e(a, b) + e(b, c) \geq e(a, c)$ .

The discussion in this appendix will focus on the last of these properties, the triangle inequality. Lagonotte ([38]) found that an electrical distance measure related to voltages generally, but not always, obeyed the triangle inequality. We demonstrate a similar finding here for an analogous distance measure which is based upon real power sensitivities. Building on [38], we also characterize the conditions under which the triangle inequality will fail to hold for this electrical distance measure.

Recall, from the discussion surrounding (13), that the sensitivity matrix  $\mathbf{G}$  is replaced with  $[\partial \mathbf{P} / \partial \theta]$  from the power flow Jacobian. In the dc power flow model [45], this sensitivity is simply equal to the system susceptance matrix  $\mathbf{B}$ . For an arbitrary, connected three-node network, following (13), the electrical distance matrix  $\mathbf{E}$  can be written as:

$$\begin{bmatrix} 0 & \frac{x_{12}(x_{13}+x_{23})}{x_{12}+x_{13}+x_{23}} & \frac{x_{13}(x_{12}+x_{23})}{x_{12}+x_{13}+x_{23}} \\ \frac{x_{12}(x_{13}+x_{23})}{x_{12}+x_{13}+x_{23}} & 0 & \frac{x_{23}(x_{12}+x_{13})}{x_{12}+x_{13}+x_{23}} \\ \frac{x_{13}(x_{12}+x_{23})}{x_{12}+x_{13}+x_{23}} & \frac{x_{23}(x_{12}+x_{13})}{x_{12}+x_{13}+x_{23}} & 0 \end{bmatrix} \quad (18)$$

Applying the triangle inequality to (18), for each of the three triplets, leads to the following sufficient condition on the three reactances:

$$\begin{aligned} & (x_{12}x_{23} \geq 0 \cap (x_{12} + x_{23} + x_{13}) > 0) \cup \\ & (x_{12}x_{23} < 0 \cap (x_{12} + x_{23} + x_{13}) < 0) \end{aligned}$$

which is clearly satisfied for a strictly positive set of reactances. Figure 7 shows the surface in  $x_{12}, x_{13}, x_{23}$  space where violations of the triangle inequality are observed, for all combinations of  $x_{ab} \in [-1, 1]$ . Areas of the surface where  $e(a, b) + e(b, c) - e(a, c) < 0$  were shaded, showing combinations of  $x_{12}, x_{13}, x_{23}$  that yielded Triangle Inequality violations. Otherwise, if one or more of the branch reactances is less than zero, a violation may occur.

## Acknowledgment

This work is supported in part by the US National Science Foundation (award #0848247) and in part by the US Department of Energy (award #DE-OE0000447). Special thanks are due to Mahendra Patel, and other staff members at PJM Applied Solutions, for providing substantial technical advice related to this effort.

- 
- [1] P. Erdos and A. Renyi, "On random graphs," *Publ. Math. Debrecen*, vol. 6, pp. 290–297, 1959.
  - [2] A.-L. Barabasi and R. Albert, "Emergence of scaling in random networks," *Science*, vol. 286, pp. 509–512, 1999.
  - [3] D. J. Watts and S. H. Strogatz, "Collective dynamics of 'small-world' networks," *Nature*, vol. 393, pp. 440–442, 1998.
  - [4] S. Boccaletti, V. Latora, Y. Moreno, M. Chavez, and D.-U. Hwang, "Complex networks: Structure and dynamics," *Physics Reports*, no. 424, pp. 175–308, 2006.
  - [5] R. Albert, H. Jeong, and A.-L. Barabasi, "Error and attack tolerance of complex networks," *Nature*, vol. 406, pp. 378–382, 2000.
  - [6] X. Wang and G. Chen, "Synchronization in scale-free dynamical networks: robustness and fragility," *Circuits and Systems I: Fundamental Theory and Applications, IEEE Transactions on*, vol. 49, no. 1, pp. 54–62, 2002.
  - [7] X. Li, X. Wang, and G. Chen, "Pinning a complex dynamical network to its equilibrium," *Circuits and Systems I: Regular Papers, IEEE Transactions on*, vol. 51, no. 10, pp. 2074–2087, 2004.
  - [8] T. Chen, X. Liu, and W. Lu, "Pinning complex networks by a single controller," *IEEE Transactions on Circuits and Systems I: Regular Papers*, vol. 54, no. 6, pp. 1317 – 1326, 2007.

- [9] F. Atay, T. Biyikoglu, and J. Jost, “Synchronization of networks with prescribed degree distributions,” *Circuits and Systems I: Regular Papers, IEEE Transactions on*, vol. 53, no. 1, pp. 92–98, 2006.
- [10] C. Wu and L. Chua, “Synchronization in an array of linearly coupled dynamical systems,” *Circuits and Systems I: Fundamental Theory and Applications, IEEE Transactions on*, vol. 42, no. 8, pp. 430–447, 1995.
- [11] C. Wu, “Synchronization in networks of nonlinear dynamical systems coupled via a directed graph,” *Nonlinearity*, vol. 18, p. 1057, 2005.
- [12] P. De Lellis, M. di Bernardo, and F. Garofalo, “Synchronization of complex networks through local adaptive coupling,” *Chaos: An Interdisciplinary Journal of Nonlinear Science*, vol. 18, p. 037110, 2008.
- [13] P. De Lellis, M. di Bernardo, F. Garofalo, and M. Porfiri, “Evolution of complex networks via edge snapping,” *Circuits and Systems I: Regular Papers, IEEE Transactions on*, vol. 57, no. 8, pp. 2132–2143, 2010.
- [14] I. Dobson, B. Carreras, V. Lynch, and D. Newman, “Complex systems analysis of series of blackouts: cascading failure, critical points, and self-organization,” *Chaos: An Interdisciplinary Journal of Nonlinear Science*, vol. 17, p. 026103, 2007.
- [15] L. A. N. Amaral, A. Scala, M. Barthelemy, and H. E. Stanley, “Classes of small-world networks,” *Proceedings of the National Academies of Science*, vol. 97, no. 21, pp. 11 149–11 152, Apr 2000.
- [16] R. Albert, I. Albert, and G. Nakarado, “Structural vulnerability of the north american power grid,” *Physical Review E*, vol. 69, no. 2, FEB 2004.
- [17] D. Chassin and C. Posse, “Evaluating north american electric grid reliability using the barabási-albert network model,” *Physica A*, vol. 355, pp. 667 – 677, 2005.
- [18] P. Crucitti, V. Latora, and M. Marchiori, “Topological analysis of the italian electric power grid,” *Physica A*, vol. 338, pp. 92 – 97, 2004.
- [19] Å. J. Holmgren, “Using graph models to analyze the vulnerability of electric power networks,” *Risk Analysis*, vol. 26, no. 4, pp. 955 – 969, Sep 2006.
- [20] R. Sole, M. Rosas-Casals, B. Corominas-Murtra, and S. Valverde, “Robustness of the european power grids under intentional attack,” *Physical Review E*, vol. 77, 2008.
- [21] Z. Wang, A. Scaglione, and R. Thomas, “Generating statistically correct random topologies for testing smart grid communication and control networks,” *Smart Grid, IEEE Transactions*

- on, vol. 1, no. 1, pp. 28–39, 2010.
- [22] P. Hines, E. Cotilla-Sanchez, and S. Blumsack, “Do topological models provide good information about vulnerability in electric power networks?” *Chaos: An interdisciplinary journal of non-linear science*, vol. 20, no. 3, 2010.
  - [23] P. Hines and S. Blumsack, “A centrality measure for electrical networks,” *Proceedings of the 41st. Hawaii International Conference on System Sciences*, 2008.
  - [24] P. Hines, S. Blumsack, E. C. Sanchez, and C. Barrows, “The topological and electrical structure of power grids,” in *Proceedings of the 43rd Hawaii International Conference on System Sciences*, 2010.
  - [25] E. Bompard, R. Napoli, and F. Xue, “Analysis of structural vulnerabilities in power transmission grids,” *International Journal of Critical Infrastructure Protection*, 2009.
  - [26] S. Arianos, E. Bompard, A. Carbone, and F. Xue, “Power grids vulnerability: a complex network approach,” *Chaos*, vol. 19, 2009.
  - [27] S. Blumsack, L. Lave, and M. Ilic, “A quantitative analysis of the relationship between congestion and reliability in electric power networks,” *Energy Journal*, vol. 28, pp. 101–128, 2007.
  - [28] D. Ming and H. Ping-ping, “Small-world topological model based vulnerability assessment algorithm for large-scale power grid [j],” *Automation of Electric Power Systems*, vol. 8, 2006.
  - [29] V. Rosato, S. Bologna, and F. Tiriticco, “Topological properties of high-voltage electrical transmission networks,” *Electric Power Systems Research*, vol. 77, no. 2, pp. 99–105, 2007.
  - [30] L. Fu, W. Zhang, S. Xiao, Y. Li, and S. Guo, “Vulnerability assessment for power grid based on small-world topological model,” in *Power and Energy Engineering Conference (APPEEC), 2010 Asia-Pacific*, 2010.
  - [31] M. Rosas-Casals, S. Valverde, and R. Solé, “Topological vulnerability of the european power grid under errors and attacks,” *International Journal of Bifurcation and Chaos*, vol. 17, no. 7, pp. 2465–2475, 2007.
  - [32] PSTCA. (2007) Power Systems Test Case Archive, University of Washington, Electrical Engineering. online: <http://www.ee.washington.edu/research/pstca/>. [Online]. Available: <http://www.ee.washington.edu/research/pstca/>
  - [33] R. Albert and A. Barabasi, “Statistical mechanics of complex networks,” *Reviews of Modern Physics*, vol. 74, 2002.
  - [34] M. E. J. Newman, “Assortative mixing in networks,” *Phys. Rev. Lett.*, vol. 89, no. 20, 2002.

- [35] —, “Mixing patterns in networks,” *Physical Review E*, vol. 67, no. 2, 2003.
- [36] A. Clauset, C. R. Shalizi, and M. E. J. Newman, “Power-law distributions in empirical data,” Arxiv working paper, 2008.
- [37] R. D. Zimmerman, C. E. Murillo-Sánchez, and R. J. Thomas, “Matpower: Steady-state operations, planning and analysis tools for power systems research and education,” *IEEE Transactions on Power Systems*, vol. 26, no. 1, pp. 12–19, Feb. 2011.
- [38] P. Lagonotte, J. Sabonnadiere, J.-Y. Leost, and J.-P. Paul, “Structural analysis of the electrical system: application to secondary voltage control in france,” *IEEE Transactions on Power Systems*, vol. 4, no. 2, pp. 479–486, May 1989.
- [39] Q. Lu and S. Brammer, “A new formulation of generator penalty factors,” *IEEE Transactions on Power Systems*, vol. 10, no. 2, pp. 990–994, May 1995.
- [40] L. Hang, A. Bose, and V. Venkatasubramanian, “A fast voltage security assessment method using adaptive bounding,” *IEEE Transactions on Power Systems*, vol. 15, no. 3, pp. 1137–1141, Aug. 2000.
- [41] J. Zhong, E. Nobile, A. Bose, and K. Bhattacharya, “Localized reactive power markets using the concept of voltage control areas,” *IEEE Transactions on Power Systems*, vol. 19, no. 3, pp. 1555–1561, Aug. 2004.
- [42] W. Rudin, *Principles of mathematical analysis*. McGraw-Hill New York;, 1964, vol. 1976.
- [43] I. Dobson, M. Parashar, and C. Carter, “Combining phasor measurements to monitor cutset angles,” in *Proc. of the 43rd Hawaii International Conference on System Sciences*, Kauai, HI, Jan. 2010.
- [44] D. Klein and M. Randic, “Resistance distance,” *Journal of Mathematical Chemistry*, vol. 12, pp. 81–95, 1993.
- [45] B. Stott, J. Jardim, and O. Alsac, “Dc power flow revisited,” *IEEE Transactions on Power Systems*, vol. 24, no. 3, pp. 1290 – 1300, 2009.
- [46] The US power grid data used in this paper were obtained through the U.S. Critical Energy Infrastructure Information (CEII) request process (Federal Energy Regulatory Commission, Online: <http://www.ferc.gov/legal/ceii-foia/ceii.asp>).

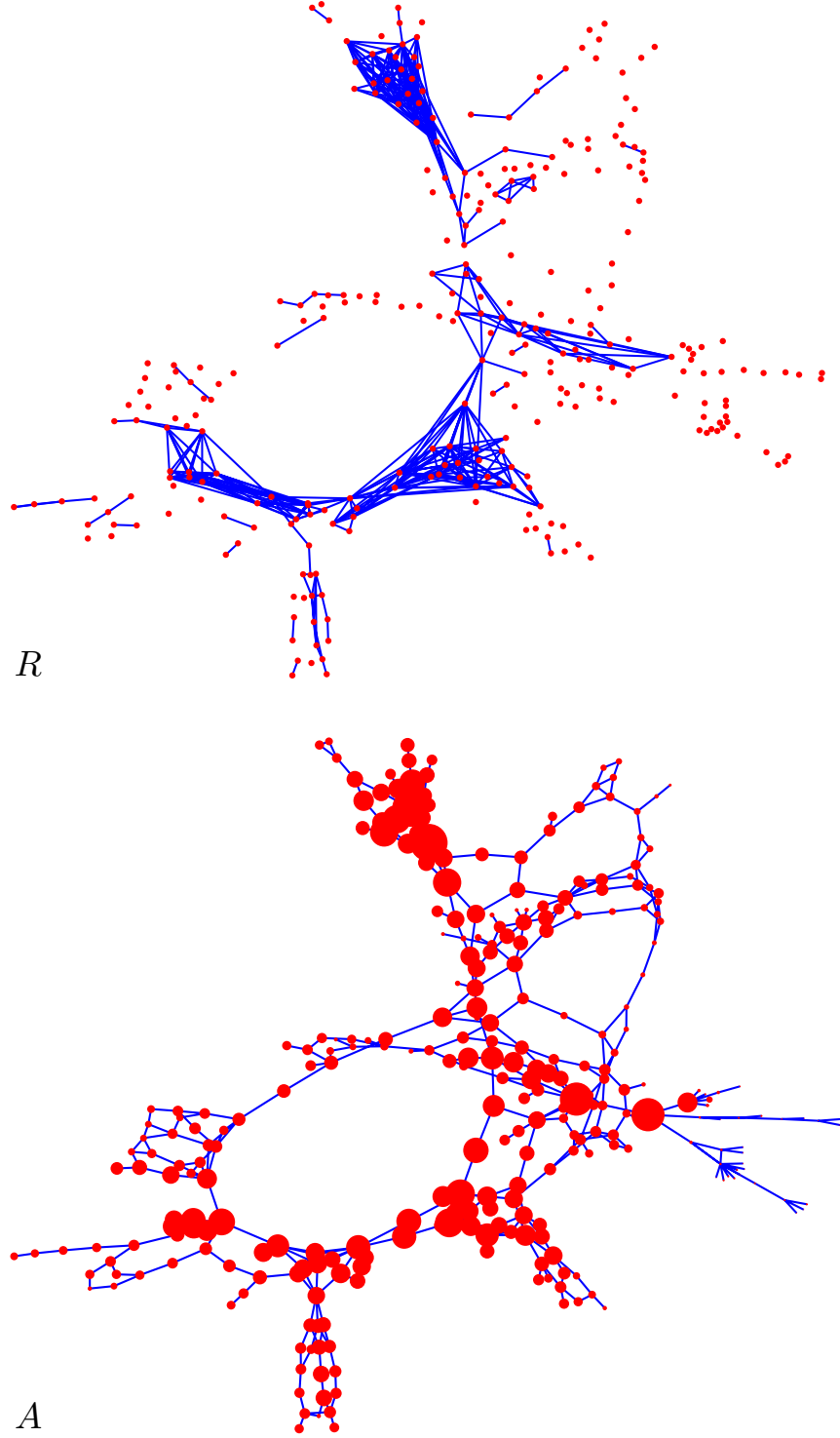


Figure 3: The upper panel shows a graphical representation of the electrical topology of the IEEE 300 bus system ( $\mathbf{R}$ ), formed by replacing the 409 transmission branches with 409 shortest distance electrical links (the 409 smallest  $e_{ij}$  such that  $i > j$ ). The lower panel shows the topology ( $\mathbf{A}$ ) of the 300 bus network with nodes drawn with sizes proportional to their electrical centrality (17).

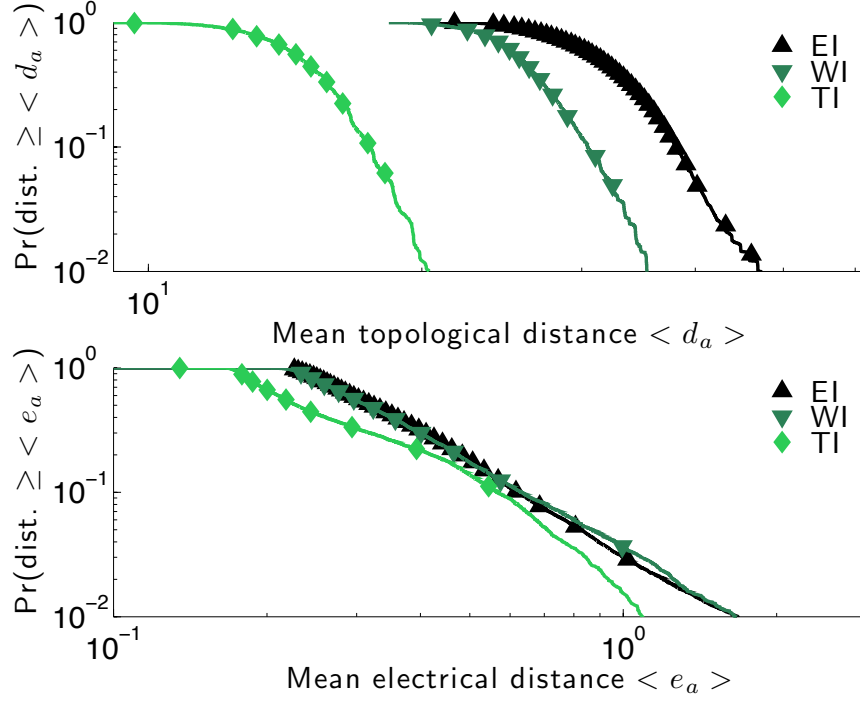


Figure 4: Complementary cumulative probability distributions for electrical and topological distances ( $d_{ab}$  and  $e_{ab}$ ) for the US Eastern, Western and Texas Interconnections. For the three distributions of topological distances, hypothesis 2 (see Section II D) is rejected\*\*. For the two larger distributions of electrical distances (EI and WI), hypothesis 2 is not rejected and the estimates of  $\alpha$  are:  $\alpha_{EI} = 3.49$  and  $\alpha_{WI} = 3.36$ . For the distribution of electrical distances in TI, hypothesis 2 is rejected\*\*. (\*\* Significant at the 0.001 confidence level.)

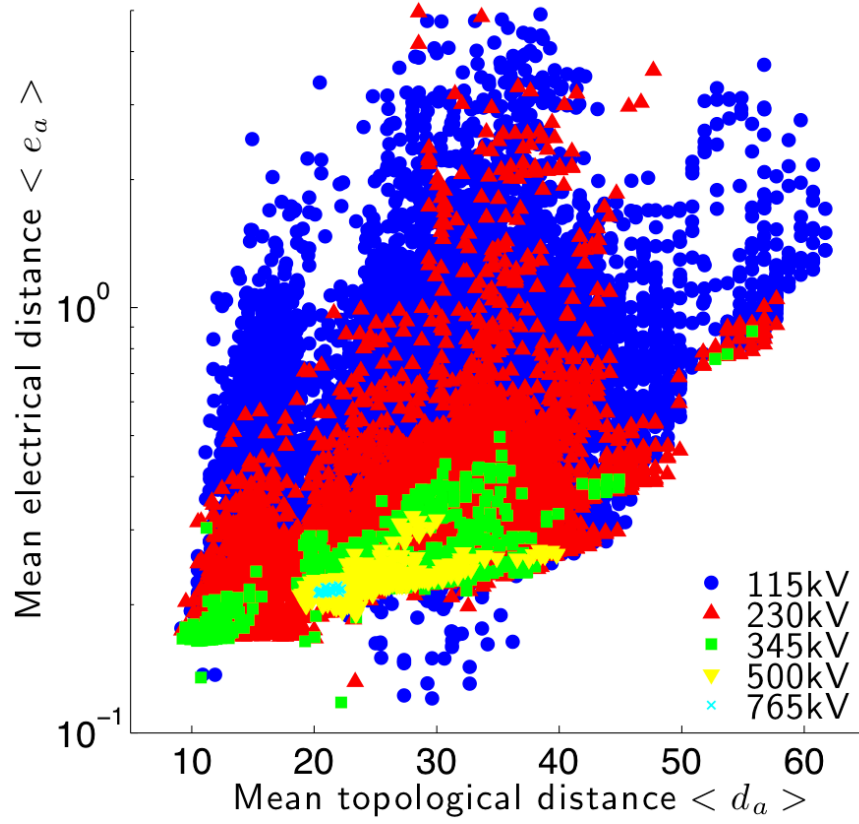


Figure 5: The mean topological and electrical distances of buses, at different voltage levels, within the three North American power networks (EI, WI and TI). The average correlation between topological distance and electrical distance is low ( $\rho = 0.24$ ), however the correlation at the higher voltage levels ( $\rho_{765} = 0.43$ ,  $\rho_{500} = 0.65$ ) is higher.



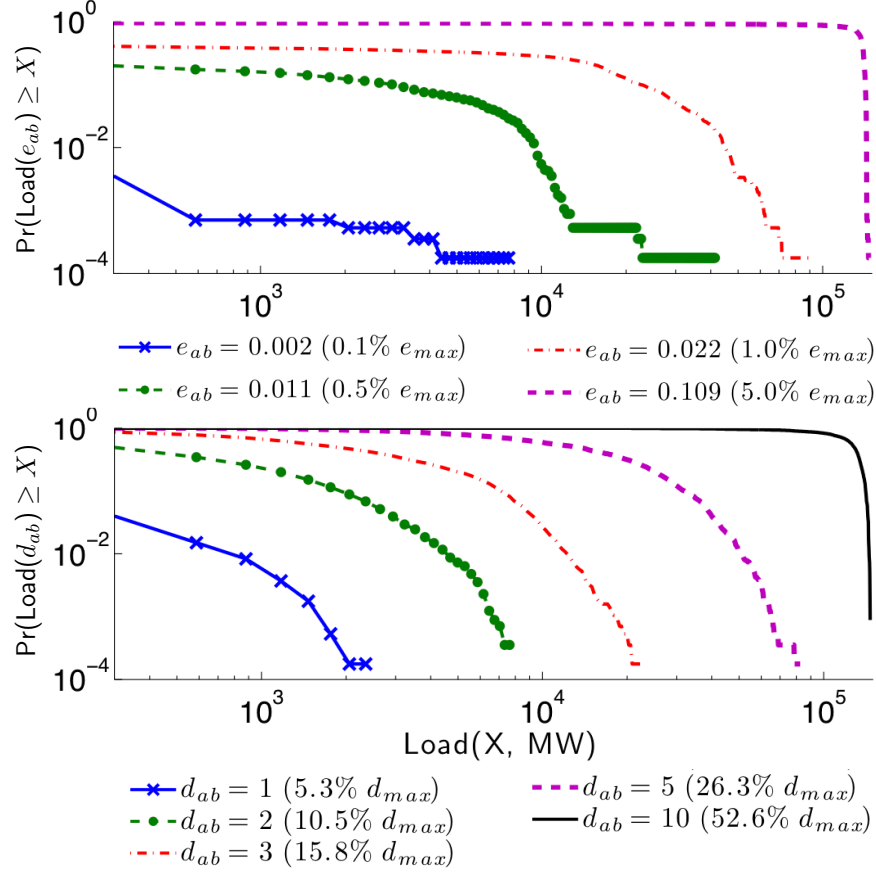


Figure 6: Electrical distances to loads for the PJM portion of the US Eastern Interconnect. The horizontal axis shows load in MW. The vertical axis for the top panel shows the probability of a randomly selected node reaching  $X$  MW of load within electrical distance  $e_{ab}$ . The lower panel shows the same result for topological distances. Electrically, we find a small number of nodes that are very highly connected to loads in the system, despite being relatively distant from loads in a topological sense.

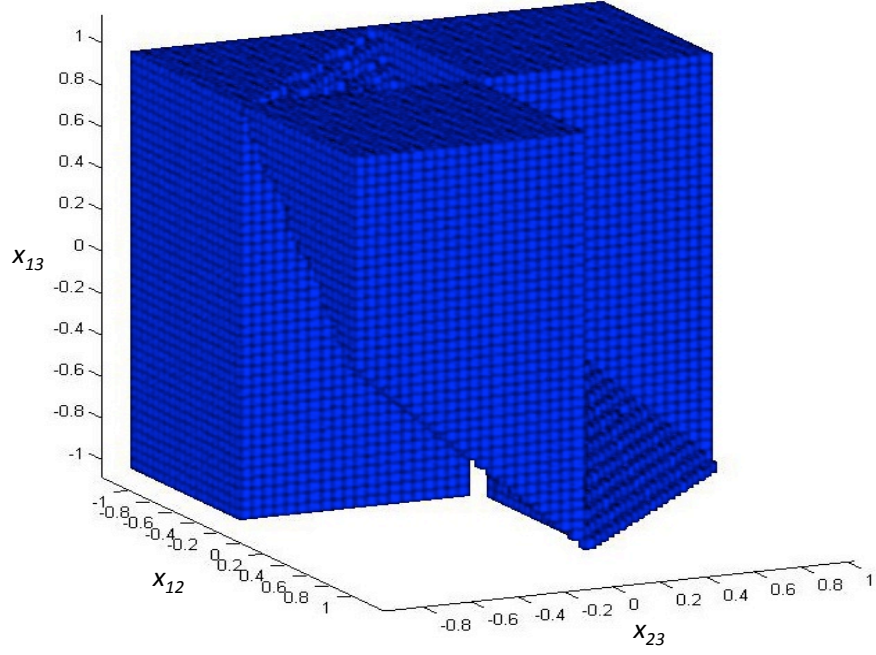


Figure 7: Illustration of the conditions under which three reactances  $(x_{ab}, x_{bc}, x_{ac})$  connecting a three-bus network satisfy the triangle inequality. Combinations that result in a triangle inequality violation are shaded.